UNCLASSIFIED

NRL Report 8694

Aperture Efficiency Considerations in the Convolution Synthesis of Symmetrical Hexagonal Arrays

J. P. SHELTON

Electromagnetics Branch
Radar Division

S. R. LAXPATI

Department of Electrical Engineering and Computer Science
University of Illinois at Chicago
Chicago, Illinois

August 31, 1983

NAVAL RESEARCH LABORATORY
Washington, D.C.

Approved for public release; distribution unlimited.

UNCLASSIFIED

REPORT DOCUMENTATION PAGE

READ INSTRUCTIONS BEFORE COMPLETING FORM

1. REPORT NUMBER
NRL Report 8694

2. GOVT ACCESSION NO.

3. RECIPIENT'S CATALOG NUMBER

4. TITLE (and Subtitle)
APERTURE EFFICIENCY CONSIDERATIONS IN THE CONVOLUTION SYNTHESIS OF SYMMETRICAL HEXAGONAL ARRAYS

5. TYPE OF REPORT & PERIOD COVERED
Interim report on continuing NRL problem

6. PERFORMING ORG. REPORT NUMBER

7. AUTHOR(s)
J. P. Shelton and S. R. Laxpati*

8. CONTRACT OR GRANT NUMBER(s)

9. PERFORMING ORGANIZATION NAME AND ADDRESS
Naval Research Laboratory
Washington, DC 20375

10. PROGRAM ELEMENT, PROJECT, TASK AREA & WORK UNIT NUMBERS
61153N; RR-021-05-43
53-1783-0-3

11. CONTROLLING OFFICE NAME AND ADDRESS
Office of Naval Research
Washington, DC 22217

12. REPORT DATE
August 31, 1983

13. NUMBER OF PAGES
26

14. MONITORING AGENCY NAME & ADDRESS(if different from Controlling Office)

15. SECURITY CLASS. (of this report)
UNCLASSIFIED

15a. DECLASSIFICATION/DOWNGRADING SCHEDULE

16. DISTRIBUTION STATEMENT (of this Report)
Approved for public release; distribution unlimited.

17. DISTRIBUTION STATEMENT (of the abstract entered in Block 20, if different from Report)

18. SUPPLEMENTARY NOTES
*Department of Electrical Engineering and Computer Science, University of Illinois at Chicago, Chicago, Illinois.

19. KEY WORDS (Continue on reverse side if necessary and identify by block number)
Radiation patterns
Synthesis
Antennas
Arrays

20. ABSTRACT (Continue on reverse side if necessary and identify by block number)

The investigation of the application of null synthesis procedures to planar arrays, described in previous reports by these authors, is continued. The null synthesis of symmetrical hexagonal arrays is evaluated in terms of the maximum achievable aperture illumination efficiency (AIE). Computed values of maximum AIE are presented for hexagonal arrays of 7, 19, 37, 61, and 91 elements using 7-element, 1-parameter canonical arrays (referred to as H_7). A 19-element 3-parameter canonical array is introduced (H_{19}), and maximum AIE is given for arrays of 19, 37,

(Continued)

DD FORM 1 JAN 73 1473 EDITION OF 1 NOV 65 IS OBSOLETE
S/N 0102-014-6601

20. ABSTRACT (Continued)

61, and 91 elements. Contour plots of radiation patterns, showing zero loci and sidelobe levels are presented for both uniformly illuminated and synthesized maximum AIE arrays. Zero loci, sidelobe levels, and aperture illumination distributions are compared for these arrays.

UNCLASSIFIED

CONTENTS

INTRODUCTION 1

OBJECTIVES OF CONVOLUTION SYNTHESIS 2

Background 2
Specific Objectives of this Report 3

ANALYSIS OF CANONICAL ARRAYS 3

COMPUTATION OF MAXIMUM AIE FOR CONVOLVED ARRAYS 7

PLOTS OF PATTERNS 11

CONCLUSIONS 18

ACKNOWLEDGMENT 21

REFERENCES 21

APPENDIX—Relationship Between AIE and the Mean Level of the Random Sidelobes 22

UNCLASSIFIED

APERTURE EFFICIENCY CONSIDERATIONS IN THE CONVOLUTION SYNTHESIS OF SYMMETRICAL HEXAGONAL ARRAYS

INTRODUCTION

Synthesis of regular hexagonal arrays has been described by several authors during the past decade. Recently, the authors of this report have investigated hexagonal array synthesis in which small arrays are convolved to synthesize large arrays. Such a technique is well suited to synthesize a set of prescribed nulls of a large array. This is a report on the status of the ongoing work by the authors.

Aside from the use of separable illumination for a planar array, which thereby utilizes well known synthesis procedures for linear arrays, a synthesis technique that has been studied extensively is based on a transformation technique that maps a linear array into a planar array. The technique was presented by Baklanov [1] and by Tseng and Cheng [2] for square arrays and was later adapted for rectangular arrays by Goto [3,4]. Since the transformation maps a 2-dimensional (θ, ϕ) pattern of a planar array into a 1-dimensional (θ) pattern of a linear array, the resultant pattern has ring sidelobes (whose heights are independent of θ) with noncircular contours. Furthermore, the technique fundamentally synthesizes a linear array; thus, it enables one to use any of the optimal or nonoptimal synthesis techniques for linear arrays. Elliott [5] extended the technique to synthesize arbitrary sidelobe topography. Goto [3,6] has discussed the application of this transformation technique to hexagonal arrays, whereas Goto [7] and Cheng and Chen [8] have treated optimal synthesis of regular hexagonal arrays. In order to synthesize a k-ring hexagonal array, synthesis of a $(2k + 1)$ element linear array is needed. Thus, in the synthesis procedure there are at most k degrees of freedom; i.e., up to k different parameters may be specified to control the hexagonal array pattern.

Although the transformation synthesis procedure is straightforward, it is rather cumbersome; the voltage excitations of the planar array are obtained from those of the corresponding linear array after extensive numerical computation which is reminiscent of the computation of coefficients n Chebyshev synthesis. Furthermore, it is difficult to provide any intuitive understanding of the null loci as well as illumination (voltage) tapers. The examples discussed by the researchers would indicate no simple relationship to the voltage tapers of the corresponding linear array. This is contrary to what one would have expected from the technique. To be specific, if a Taylor type illumination and sidelobe structure is used as a linear array design, then although the sidelobes of the hexagonal array will have similar structure in all azimuth planes, the aperture illumination will not exhibit the behavior of the corresponding linear array illumination. The synthesis procedure yields a twelvefold symmetry in the aperture plane, a feature that is analogous to the rotational symmetry of 1-dimensional circular Taylor illumination. Thus, the synthesis of a hexagonal array may be thought of as an extension of the 1-dimensional circular aperture synthesis to two dimensions.

The synthesis procedure for hexagonal arrays described by Einarsson [9] retains the symmetry requirements. The procedure is numerical and is capable of providing optimal patterns (i.e., optimizes aperture illumination efficiency (AIE) for a fixed sidelobe level). The problem is formulated as a quadratic programming problem and requires a number of iterations and a large computer to obtain the solution.

Shelton [10] studied regular hexagonal arrays in depth and considered a synthesis procedure in which small hexagonal arrays are convolved to synthesize large hexagonal arrays but was confined to

Manuscript approved January 20, 1983.

one degree of freedom which leads to hexagonal arrays with binomial voltage excitations and twelvefold symmetry. Laxapti [11,12] introduced a null synthesis technique for planar arrays, which is based on the convolution process and is a generalization of the previous synthesis procedure. This procedure, which utilized a canonical 4-element diamond array, can be utilized to synthesize prescribed arbitrary nulls and/or sidelobe topography. For a *k*-ring hexagonal array, the procedure has no more than 1.5 k degrees of freedom.

An important characteristic of this null synthesis procedure is that it is noniterative and can be readily implemented on a small computer. It also provides a larger number of degrees of freedom than the transformation synthesis procedure. In an attempt to evaluate the potential of the null synthesis procedure, the present authors presented a study [13,14] which introduces the canonical arrays and discusses their role in the synthesis of various planar arrays including regular hexagonal arrays. The results indicated that AIE is dependent on the canonical arrays employed to synthesize the large array; it is also dependent on the number of degrees of freedom. Since AIE is the ratio of the directivity of the designed antenna excitation to the directivity of uniform excitation, it would be an important criterion in the selection of canonical arrays, if not constrained by the symmetry requirements.

The primary objective of this report is to consider the null synthesis procedure for hexagonal arrays with twelvefold symmetry (thus employing smaller hexagonal arrays as canonical arrays) and optimize the AIE. Syntheses of hexagonal arrays with 2, 3, 4 and 5 rings are considered. In the next section, after reviewing the convolution (null) synthesis technique, symmetry and other characteristics of hexagonal arrays are introduced. More detailed objectives are also put forth. Then we analyze the 1- and 2-ring (7- or 19-element) hexagonal arrays which are used as canonical arrays in the synthesized examples presented. Also discussed is the simple technique used to achieve the near optimum value of AIE as well as the impact on it of using H_7 (7-element, 1-ring hexagonal array) and H_{19} (19-element, 2-ring hexagonal array) as building blocks. Then we show the plots of patterns of the synthesized arrays and compare them with those of uniform arrays. Finally, some concluding remarks are offered.

OBJECTIVES OF CONVOLUTION SYNTHESIS

Background

This investigation of a convolution synthesis procedure for planar arrays was initiated because there were no zero-locus synthesis procedures analogous to those which are commonly used for linear arrays. In contrast with the polynomial representation of linear arrays which allows the pattern function to be expressed in terms of its roots, there is no mathematical formalism which allows the pattern function of a planar array to be expressed in terms of its zero loci. This situation is not surprising because, whereas a linear array has a finite set of zeros which can be related to the coefficients of the polynomial describing the pattern function, the symmetrical planar arrays being considered here have continuous zero loci with an infinite number of locations, and their pattern functions are not expressible as polynomials. On the other hand, the concept of array convolution and pattern multiplication still holds.

This concept of array convolution and pattern multiplication has been proposed by these authors in previous papers. It is in effect what such procedures as Taylor's do, without relating the zero locations to the pattern function expressions. For example, an alternative approach to the Taylor synthesis would relate the pattern zeros to small 2- or 3-element arrays and then convolve them to determine the overall array excitation directly without being concerned about the polynomial expression.

The objective of this convolution synthesis is to select appropriate small arrays, which we will refer to as canonical, determine their zero loci from a number of small arrays to give a desired multiplied pattern from a large array, and finally convolve the small arrays to determine the array distribution of the large array.

UNCLASSIFIED

This procedure is not without drawbacks. Whereas the linear-array zero locus procedures such as Taylor's tend to produce array excitations with good aperture efficiency, this is not necessarily the case with planar arrays. One of the primary objectives of the analysis of this technique is to evaluate the aperture efficiency with which patterns of given sidelobe levels can be synthesized. Furthermore, there is not a readily available procedure for relating the zero loci to a given specified sidelobe level, as is the case for Taylor's and Dolph's techniques.

Therefore, the present status of this investigation is to seek answers to the questions of exactly how well will the convolution procedure work and what is a specific technique for selecting the required zero loci.

Specific Objectives of this Report

One specific objective of this report is to analyze and present the pattern characteristics of uniform symmetrical hexagonal arrays as large as 91 elements. A disadvantage of dealing with planar arrays with nonseparable pattern functions is that the characteristics of those patterns are not generally familiar to workers in the field. Essentially anyone reading this report will know what a $\sin Nx/\sin x$ pattern function looks like and that it is the pattern of a uniform N-element linear array. How many of us know how to describe even qualitatively the characteristics of a uniform hexagonal array? Locations and levels of sidelobes will be presented, and zero loci will be plotted.

Characteristics of two canonical arrays will be considered. The 7-element array with one degree of freedom has been analyzed previously. The 19-element array with three degrees of freedom is analyzed, and procedures for determining the array coefficients in terms of specified zero locations or vice versa will be discussed.

Using these canonical arrays, arrays as large as 91 elements will be synthesized for maximum aperture efficiency (AIE), and the radiation patterns, aperture distributions, and zero loci of these arrays will be presented and compared with those of the uniform arrays.

ANALYSIS OF CANONICAL ARRAYS

The zero-locus characteristics of two canonical arrays are analyzed in this section. The first is the 1-parameter 7-element array (H_7) and the second is the 3-parameter 19-element array (H_{19}). The 7-element array geometry is shown in Fig. 1.

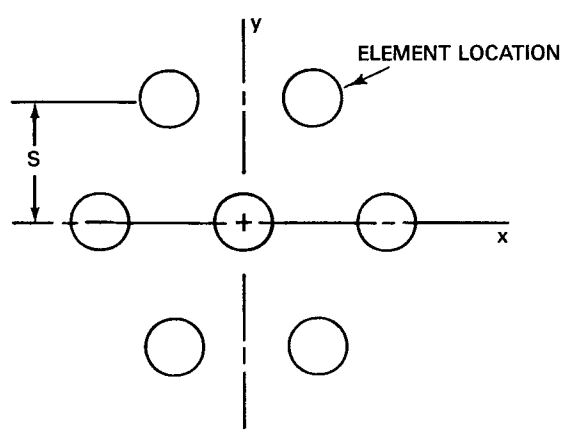

Fig. 1 — Smallest symmetric hexagonal array

The coordinate system used for representing radiation pattern functions is shown in Fig. 2. The pattern function coordinate corresponding to the x coordinate of the array is u, and the coordinate corresponding to the y coordinate of the array is v. The coordinate system is defined so that the angular distance from the mainlobe to the nearest grating lobe is 2π. Specifically, $u = (2\pi/\lambda)(\cos\theta_x)$ and $v = (2\pi/\lambda)(\cos\theta_y)$, where s is the minimum spacing between rows of elements and θ_x and θ_y are the angles from x and y axes respectively. A grating-lobe pattern is also shown, which results from a "stable" triangular array lattice, that is, a lattice for which the triangles have one horizontal side.

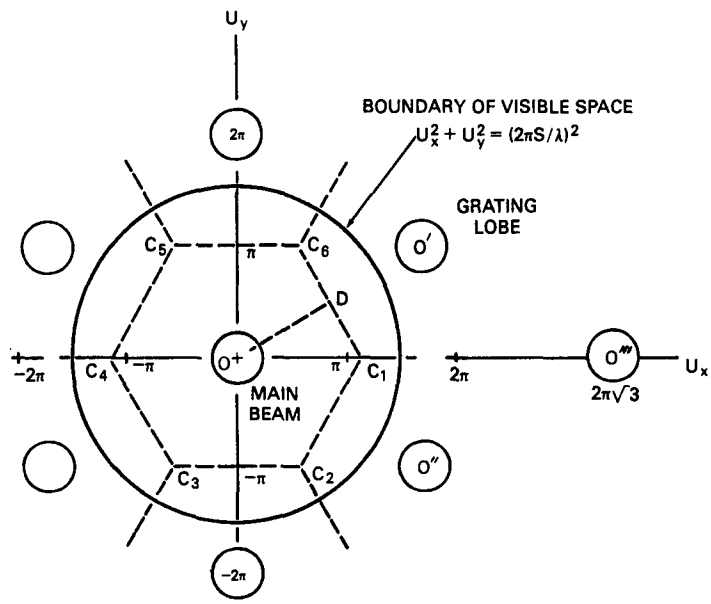

Fig. 2 — Pattern-function representation in the u-v plane

The grating-lobe pattern of Fig. 2 has the spatial periodicity of the reciprocal lattice* of the antenna-array lattice. The coordinates of the grating lobes are

$$u(m) = m\pi\sqrt{3}$$

and

$$v(m,n) = 2\pi\left(n - \frac{m}{2}\right).$$

The general pattern function for arbitrary excitation has the periodicity of the grating lobes in the $u-v$ plane, and the cell defined by the hexagon $C_1C_2C_3C_4C_5C_6$ completely describes the function. Furthermore, with the symmetry constraints which we have placed on the array, 1/12 of the cell, defined by the triangle $0C_1D$, is sufficient to completely describe the pattern functions with which we are concerned. Also shown in Fig. 2 is a circle defined by $u^2 = v^2 = (2\pi s/\lambda)^2$, which represents the boundary of visible space. The radius of this circle is directly proportional to s. The synthesis procedures considered here address the hexagonal cell without regard to any limitations imposed by s. That is, pattern functions are synthesized over the entire cell even though part of the cell could be excluded from visible space by appropriate selection of s.

*For the antenna array lattice defined by $\bar{a}_1$ and $\bar{a}_2$, the smallest pair of basis vectors greater than zero, the reciprocal lattice has the basis vectors $\bar{b}_1$ and $\bar{b}_2$ such that the inner products $(\bar{b}_i \bar{a}_k) = \delta_{ik}$, for $i = 1, 2$ and $k = 1, 2$. Here δ_{ik} is the Kronecker delta.

UNCLASSIFIED

We first consider the pattern characteristics of 7-element arrays for which the center element has unit excitation and the outer elements are excited with amplitude a. The pattern function is given by

$$E(u,v,a) = 1 + a\left[4 \cos \frac{u}{\sqrt{3}} \cos v + 2 \cos \frac{2u}{\sqrt{3}}\right], \tag{1}$$

and for values of $a < 1$ the main lobe broadens and the locus of zeros moves away from the main lobe. The zeros for the x-axis cut are given by

$$\cos \frac{u}{\sqrt{3}} = \frac{1}{2}\left[-1 \pm \sqrt{3 - \frac{1}{a}}\right] \tag{2}$$

and the zeros for the y-axis cut are given by

$$\cos v = -\frac{1 + 2a}{4a}.$$

Equations (1) and (2) can be examined to establish some limits on the ranges of a which we will investigate. Zeros for real values of v are found on the v-axis cuts for $a \geqslant 1/2$ and $a \leqslant -1/6$. Zeros are found on the u-axis for $a \geqslant 1/3$ and $a \leqslant -1/6$. For $-1/6 < a < 1/3$ the pattern function has no zeros for real u or v. These restrictions on u and v are simply due to the pattern function and are unrelated to restrictions on u and v which result from the boundary of the visible region.

Figure 3 illustrates how the locus of zeros moves with variation in the parameter a. The locus approaches 0 as $a \rightarrow -1/6$ from below, and it approaches C_1 as $a \rightarrow 1/3$ from above. It can be shown that for a near $-1/6$, $(a = -(1/6) - \epsilon)$,

$$u \approx v \approx 3\sqrt{2\epsilon} \text{ (in radians)}, \tag{3}$$

and that for a near $1/3$, $(a = 1/3 + \delta)$

$$\Delta u \approx \pm 3\sqrt{\delta}, \tag{4}$$

where $u = 2\pi/\sqrt{3} + \Delta u$. Equations (3) and (4) indicate that the locus of zeros becomes circular in the neighborhoods of 0 and C_1.

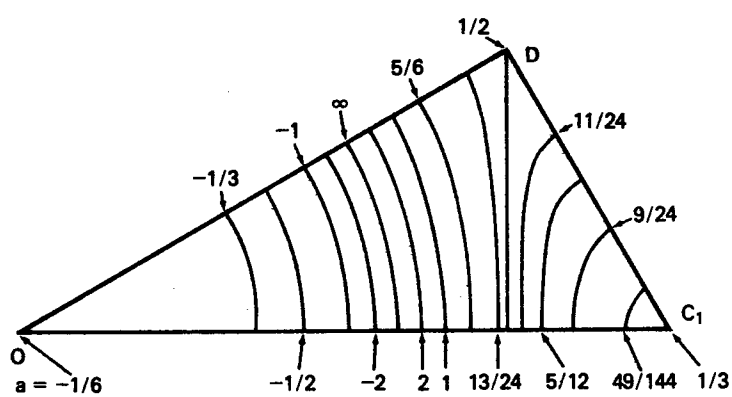

Fig. 3 — Locus of zeros for various values of a

Other characteristics of the pattern function that are of interest and easily determined are the pattern values at C_1 and D. The pattern values at 0, C_1 and D are

$$E_0 = 1 + 6a,$$

$$E_{C_1} = 1 - 3a,$$

and

$$E_D = 1 - 2a.$$

We next consider the pattern characteristics of 19-element arrays for which the center element has unit excitation and the outer elements are excited with amplitudes a, b, and c, as indicated in Fig. 4. The pattern function is given by

$$E(u,v,a,b,c) = 1 + 2a \cos \frac{2u}{\sqrt{3}} + 2b \cos \frac{4u}{\sqrt{3}} + 4 \cos v \left[a \cos \frac{u}{\sqrt{3}} + c \cos \frac{3u}{\sqrt{3}}\right] + \cos 2v \left[2c + 4b \cos \frac{2u}{\sqrt{3}}\right]. \tag{5}$$

Unlike the 7-element array, for which the zero locus is determined by the value of a and the entire family is easily plotted in Fig. 3, the 19-element array has a much more complex family of loci which cannot be easily plotted. An idea of the possible loci can be obtained by considering the behavior of $E(u,v,a,b,c)$ on the u and v axes.

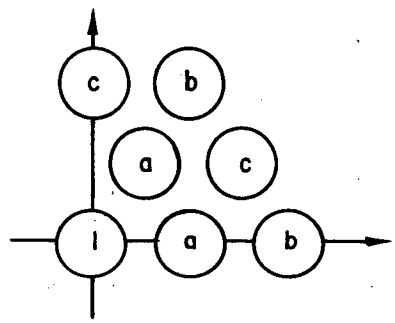

Fig. 4 — Assignment of coefficients for 19-element canonical array

On the u axis, Eq. (5) yields, for $v = 0$,

$$E(u,0,a,b,c) = 1 + 2c + 4a \cos \frac{u}{\sqrt{3}} + (2a + 4b) \cos \frac{2u}{\sqrt{3}} + 4 \cos \frac{3u}{\sqrt{3}} + 2b \cos \frac{4u}{\sqrt{3}}. \tag{6}$$

Equation (6) can be expanded into a quartic polynomial in $\cos u/\sqrt{3}$, implying that there can be four zeros in u for appropriate values of a, b, and c.

On the v axis, Eq. (5) yields, for $u = 0$,

$$E(0,v,a,b,c) = 1 + 2a + 2b + 4(a + c) \cos v + (4b + 2c) \cos 2v. \tag{7}$$

Equation (7) can be expanded into a quadratic polynomial in $\cos v$, implying that there can be two zeros in v for appropriate values of a, b, and c.

Some useful relationships for symmetrical hexagonal arrays are as follows:

$$N = 3n_r^2 + 3n_r + 1,$$

where N is the number of elements in an array with n_r rings;

$$n_e = \text{Int}\ (n_r^2/4 + n_r), \tag{8}$$

where n_e is the number of independent element voltages in an array with n_r rings.

UNCLASSIFIED

COMPUTATION OF MAXIMUM AIE FOR CONVOLVED ARRAYS

It has been noted that the number of degrees of freedom available from a hexagonal array synthesized by the convolution technique being considered here is less than the number of independent voltages which can be placed on the array, so that in general a precise synthesis cannot be achieved. That is, if we were to require a radiation pattern function to be defined as precisely as possible, then independent control of the maximum possible number of elements in the array would be required. In other words, the convolution synthesis procedure cannot realize all possible array voltage distributions. This situation raises the following important questions which must be answered before we proceed further in developing the synthesis procedure:

1. How close to any given array voltage distribution can the convolution synthesis approach?

2. Under what conditions is the synthesis procedure useful?

3. How do these answers change as the size of the array increases?

The basis for the concern for the degradation in the performance of the synthesis procedure with increasing array size is indicated by Table 1, in which the number of elements, number of rings, and number of independent element voltages are listed for various arrays.

Table 1—Some Parameters of Symmetrical Hexagonal Arrays

Number of Rings, n_r	Number of Elements, N	Number of Independent Element Voltages, n_c
1	7	1
2	19	3
3	37	5
4	61	8
5	91	11
6	127	15
7	159	19

From Eq. (8) we see that the ratio of the number of rings to the number of independent elements is

$$R_r = \frac{n_r}{\mathrm{Int}\left[\frac{n_r^2}{4} + n_r\right]} \approx \frac{4}{n_r + 4} \tag{9}$$

Equation (9) is approximate for odd n_r and precise for even n_r. If we use 7-element arrays (H_7) for the synthesis, the number of degrees of freedom is equal to n_r. If we use one 19-element array (H_{19}), the number of degrees of freedom becomes $n_r + 1$ and increases by one for each additional H_{19} that is used in the synthesis. Thus, if the number of H_{19} arrays used is m, the ratio of degrees of freedom to the number of independent elements is

$$R_f = \frac{4 + m/n_r}{4 + n_r} \tag{10}$$

Equation (10) and Table 1 need not cause us to despair of achieving a useful synthesis for larger arrays because, for example, the usefulness of a Taylor synthesis, which requires that the array have $\bar{n}$ available degrees of freedom, is independent of the size of the array. Thus, we can point to a case for which the number of degrees of freedom need not be comparable to the number of independent element voltages.

We have selected the directivity function as the basis for a figure of merit for the convolution synthesis procedure. The advantages of this choice are that the peak nonsupergain directivity of any array is readily identified as N (assuming unity element directivity), and the maximum directivity achievable from a given synthesis procedure is straightforwardly determined. A figure of merit that can be applied to arrays of all sizes is then maximum efficiency or AIE, which is the ratio of the achieved directivity to N.

We have examined the characteristics of arrays ranging in size from seven to 91 elements by applying the convolution synthesis procedure so as to maximize the AIE. Seven- (H_7) and 19-element (H_{19}) arrays were used. Initially, arrays synthesized entirely with H_7 arrays were examined. Then a synthesis procedure using one H_{19} array plus a number of H_7 arrays was tried.

Of course, the 7-element array is a trivial case for both H_7 and H_{19}, and the 19-element array is a trivial case for H_{19}.

To determine the maximum directivity available from the procedure, a straightforward hill-climbing technique was used. This technique involves the measurement of rate of change of gain with respect to all variable parameters and the use of a steepest-ascent path to the maximum gain condition. The procedure can be carried out on a programmable calculator (with some patience) or in minutes using a desk-top computer.

As is the case in many optimization techniques, the hilltop that one may achieve may be local rather than global. To avoid this pitfall, it is desirable to make judicious choices of the initial values of the parameters. This was accomplished by first evaluating the zero loci of uniformly excited hexagonal arrays, then attempting to match the zero loci of the H_7 or H_{19} arrays with those of the uniform array that we wish to approximate. For H_7, we use Eqs. (1) or (2) to determine the trial value of a for a given zero locus. For H_{19} we must select three points on the zero loci and then select from Eqs. (5), (6) and (7) in order to form a set of three simultaneous equations in a, b, and c, the solution of which will yield the desired initial values.

The steps in the analysis are as follows: The trial values of the coefficients of the various arrays being used in the convolution process are selected. The arrays are convolved to determine the element voltages for the large array. This convolution can be done either numerically after the coefficient values are selected or algebraically prior to selection of numerical values. From a computational standpoint, the use of algebraic expressions is more efficient. Once the element voltages have been determined, the directivity and efficiency are easily calculated from $D = (\Sigma E)^2/\Sigma^2$. Each coefficient is then incremented and the corresponding increment in directivity is determined, so that a steepest-ascent path to the maximum can be followed.

Table 2 lists the resulting H_7 and H_{19} coefficients for the synthesis procedures that were attempted, together with the element voltages and values of AIE. The values of AIE are plotted *vs* N in Fig. 5. Case B for the 61-element array is not included in Fig. 5 because it represents a local rather than a global maximum. The near-circular zero locus close to the main beam was synthesized with one of the H_7 arrays, indicated by $d = -0.2142$ in Table 2. It was found that the global maximum occurs when the inner two ring zero loci are synthesized with the H_{19} array. The marked imrovement that is obtained by using one H_{19} array in place of two of the H_7 arrays is readily apparent from Fig. 5.

UNCLASSIFIED

Table 2 — Parameters of Optimized Synthesized Arrays for $N = 19$ through 91

Number of Elements		19	37	37	61	61	61	91	91
Synthesis Procedure		$(H_7)^2$	$(H_7)^3$	$H_{19} * H_7$	$(H_7)^4$	$H_{19} * (H_7)^2$ Case A	$H_{19} * (H_7)^2$ Case B	$(H_7)^5$	$H_{19} * (H_7)^3$
Coefficients	H_{19} a			−0.2242		−0.2304	0.3392		−0.2108
	H_{19} b			0.5356		0.3457	0.5426		0.2775
	H_{19} c			−0.0885		−0.1945	0.2645		−0.2013
	H_7 d	−0.5750	−0.2625	0.5747	−0.2181	0.5201	−0.2142	−0.1991	−0.9159
	H_7 e	0.4100	0.4395		−0.5350	3.7858	0.5382	−0.3322	1.0647
	H_7 f		−6.645		1.0546			−1.7203	0.4904
	H_7 g				0.4016			0.6541	
	H_7 h							0.3786	
Array Element Voltages	0	−0.4145	2.453	0.2269	0.3198	0.9039	−0.2427	−0.3702	−0.2400
	1	−0.4008	2.449	0.2989	0.3191	0.8229	−0.1450	−0.3699	−0.3014
	2	−0.2358	3.309	0.3050	0.2292	0.8382	−0.1483	−0.4314	−0.3134
	3	−0.4715	2.018	0.2694	0.3646	0.9065	−0.1843	−0.3993	−0.2698
	4		0.7667	0.3078	0.4439	0.8642	−0.1104	−0.2702	−0.3070
	5		2.300	0.2569	0.3434	0.8635	−0.1975	−0.3559	−0.2684
	6				0.4941	0.6806	−0.0626	−0.4385	−0.3682
	7				0.1977	0.9783	−0.1556	−0.4856	−0.2439
	8				0.2965	0.5953	−0.1861	−0.3760	−0.3551
	9							−0.0282	−0.1327
	10							−0.1409	−0.3019
	11							−0.2019	−0.2421
AIE		0.9367	0.8973	0.9931	0.8748	0.9821	0.9341	0.8633	0.9633

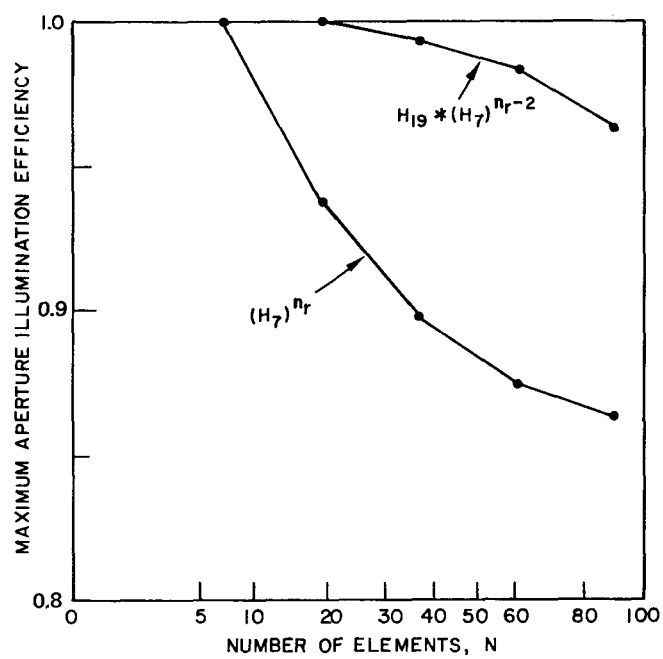

Fig. 5 — Maximum AIE *vs N*

We are encouraged to speculate that maximum AIE may be asymptotic with some value, perhaps in the range of 0.8 to 0.85, for increasing N for the $(H_7)^{n_r}$ procedure. The maximum AIE available from $H_{19} * (H_7)^{n_r-2}$ will always exceed that obtained with $(H_7)^{n_r}$, but it is impossible to estimate from Fig. 5 whether there is a separate asymptote for this case.

A qualitative idea of the relevance of these AIE optimizations can be obtained by considering the effect of reduced aperture efficiency on the radiation pattern. If the directivity reduction is due to quasi-random fluctuations in the aperture distribution, then the power contained in those fluctuations will be distributed randomly into sidelobes. Phase fluctuations would have the same effect, but we have no phase errors. To the degree that they are not controllable, these random sidelobes will limit our ability to synthesize low-sidelobe radiation patterns.

By use of this approach, the mean level of the random sidelobes can be estimated. In the Appendix, this is worked out in detail. Equation (A6) relating the sidelobe level to the AIE, is used to obtain the plot of Fig. 6.

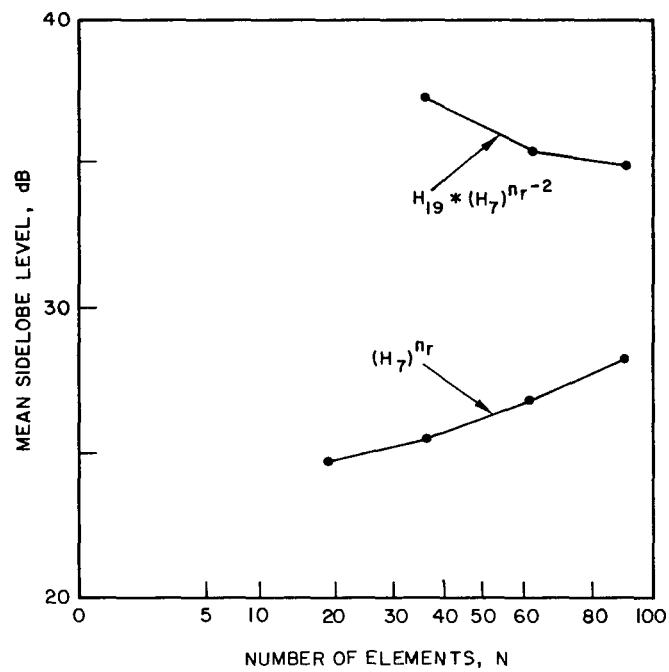

Fig. 6 — Mean level of random sidelobes *vs N*

On the other hand, it is noted that the convolution synthesis procedure can be used to achieve arbitrarily low sidelobes. For example, Shelton showed that a synthesis process of the form $(H_7)^{n_r}$, with all array coefficients equal to 1/3, compresses all zero loci to the corners of the hexagonal pattern cell and results in an aperture distribution analogous to the linear array with binomial voltages. It will be demonstrated in the next section that, in general, $(H_7)^{n_r}$ produces ring sidelobes of arbitrarily controllable height.

UNCLASSIFIED

PLOTS OF PATTERNS

The arrays synthesized and presented in the previous section exhibit a twelvefold symmetry in both aperture and pattern planes. Thus, it suffices to show the patterns in 1/12 of the hexagonal pattern cell (shown in Fig. 2). The symmetry in the pattern plane is illustrated here, in Fig. 7, for the case of a uniform H_{19} array. The normalized field pattern contours are plotted in the first quadrant of the normalized $u - v$ space. Also shown in this figure are the section of the pattern cell and the twelvefold symmetric triangular cell. The position of the main beam ($u = v = 0$) is indicated on the plot by ◇. It is clear from Fig. 7 that it is sufficient to plot the patterns in the triangular cell adjoining the coordinate axis; this will be the case in the plots that follow.

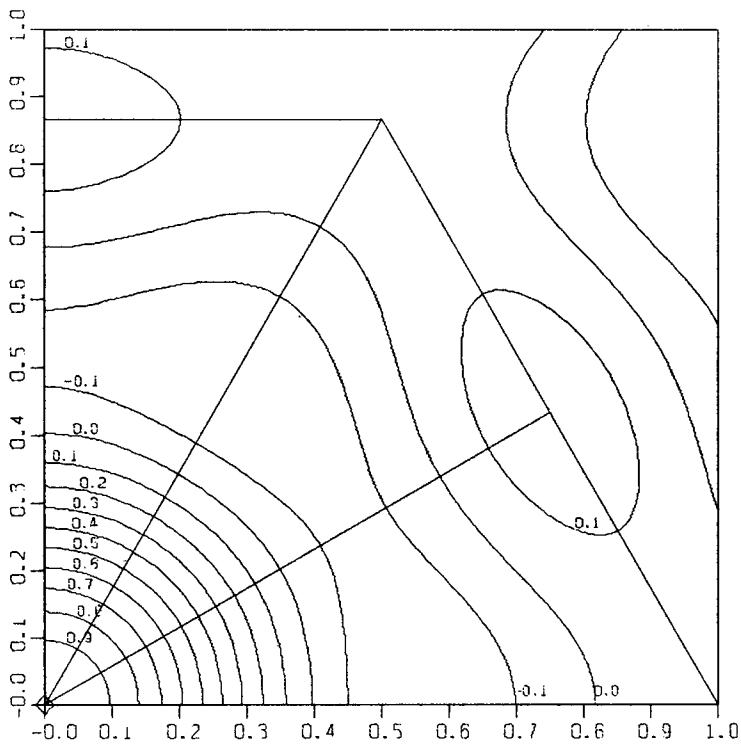

Fig. 7 — Field pattern of a uniform H_{19} array showing the symmetries and the pattern cell

For a synthesized array, there are two basic aspects that must be studied to evaluate the synthesis. One of these is the element voltages and voltage (illumination) taper; the other is the pattern structure/topography. The synthesis technique presented in this report is based on the location of pattern nulls; hence, it would be instructive to look closely at the null loci, and compare them with those of the corresponding uniform arrays. These characteristics of the synthesis are discussed in the following.

The element voltages for each of the large arrays (discussed in the previous section) are obtained by direct convolution of the element voltages of the corresponding H_7 and/or H_{19} subarrays. Due to symmetry, it is sufficient to calculate the element voltages or a small number of elements in the large array; this number is equal to the number of degrees of freedom for the array. From the subarray element voltages presented in Table 2, the voltages for the large arrays were computed; these are shown in Table 3, wherein the voltages are normalized with respect to the center element. One of the characteristics of these voltages is that it is the lowest for the outermost element; this is, of course, a direct consequence of the convolution method of synthesis. With the exception of the outermost element, the voltages vary over a 3 to 1 range.

Table 3—Element Voltages for Various Synthesized Arrays

Element No.	$H_7 * H_7$	$H_7 * H_7 * H_7$	$H_{19} * H_7$	$H_7 * H_7 * H_7 * H_7$	$H_{19} * H_7 * H_7$ Case A	$H_{19} * H_7 * H_7$ Case B	$H_7 * H_7 * H_7 * H_7 * H_7$	$H_{19} * H_7 * H_7 * H_7$
n	H_{19}	H_{37}	H_{37}	H_{61}	H_{61} *	H_{61} †	H_{91}	H_{91}
0	1.0	1.0	1.0	1.0	1.0	1.0	1.0	1.0
1	0.967	0.999	1.317	0.998	0.910	0.598	0.999	1.256
2	0.569	1.349	1.344	0.717	0.927	0.611	1.166	1.306
3	1.138	0.823	1.187	1.140	1.003	0.759	0.917	1.124
4		0.313	1.356	1.388	0.956	0.455	0.730	1.279
5		0.938	1.132	1.074	0.955	0.814	0.962	1.118
6				0.155	0.753	0.258	1.185	1.534
7				0.678	1.082	0.641	1.312	1.016
8				0.927	0.659	0.767	1.016	1.479
9							0.076	0.553
10							0.381	1.258
11							0.761	1.009

*All H_{19} zeros close to the main beam
†One H_7 zero close to the main beam

An interesting question that may be raised in optimization of the AIE is how do the null loci differ from those of the corresponding uniform array which has an AIE = 1. In Fig. 8, the null loci of a uniform H_{19} are shown along with those of the synthesized H_{19} array. The synthesized array has larger beamwidth between nulls. The null loci of uniform H_{37}, and two synthesized H_{37} arrays are shown in Fig. 9. The H_{37} array synthesized from only H_7 subarrays has larger beamwidth between nulls; however, the array synthesized using H_{19} and H_7 arrays has the first null locus identical to that of the uniform array; i.e., equal beamwidth between nulls.

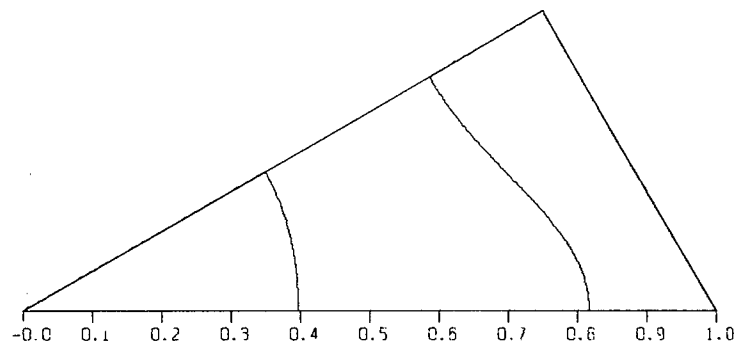

(a)

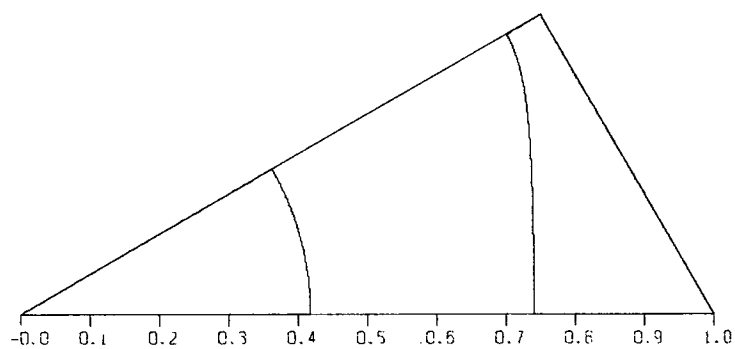

(b)

Fig. 8 — Null loci plots of H_{19} arrays:
(a) uniform (b) $H_7 * H_7$

UNCLASSIFIED

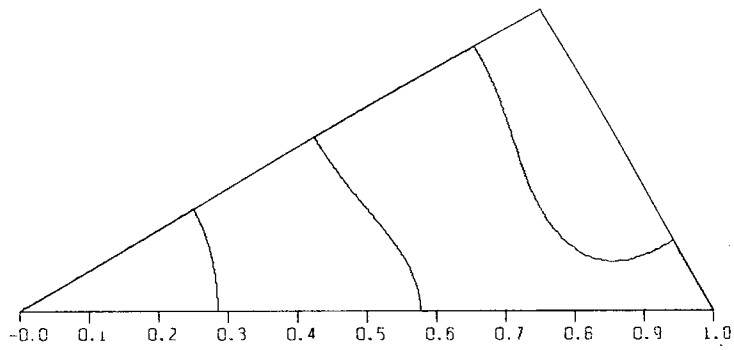

(a)

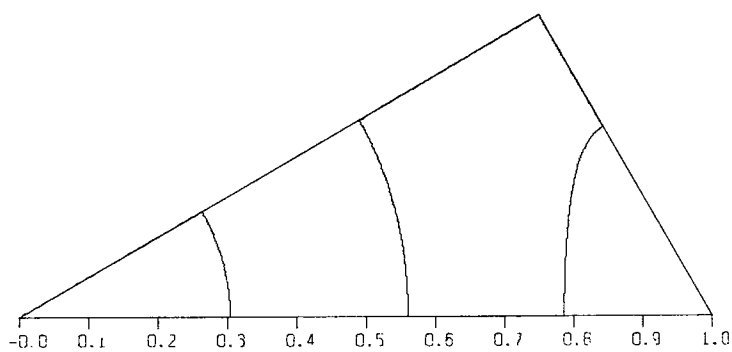

(b)

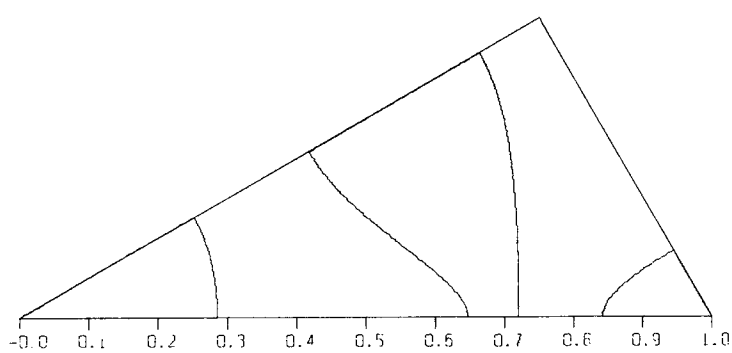

(c)

Fig. 9 — Null loci plots of H_{37} arrays: (a) uniform, (b) $H_7 * H_7 * H_7$ and (c) $H_{19} * H_7$

The null loci of H_{61} arrays are shown in Fig. 10; for the uniform array in Fig. 10a; for the array convolved from four H_7 arrays in Fig. 10b; or the array convolved from H_{19} and two H_7 arrays, where all zeros of the H_{19} are near the main beam, in Fig. 10c; and in Fig. 10d for the array convolved with one H_7 subarray zero near the main beam. The beamwidth between nulls for Figs. 10b and d is larger than and for Fig. 10c equal to that of the uniform array in Fig. 10a. Figure 11 shows the null loci for three different H_{91}. The beamwidth between nulls for Fig. 11b, the array synthesized from five H_7 elements, is larger than that of the uniform array in Fig. 11a. The array synthesized with one H_{19} and three H_7 elements has the first two null loci (Fig. 11c) identical to those of the uniform array.

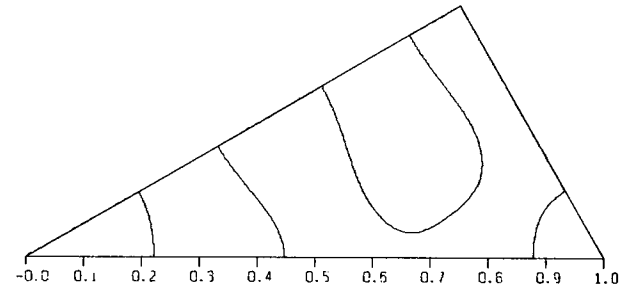

(a)

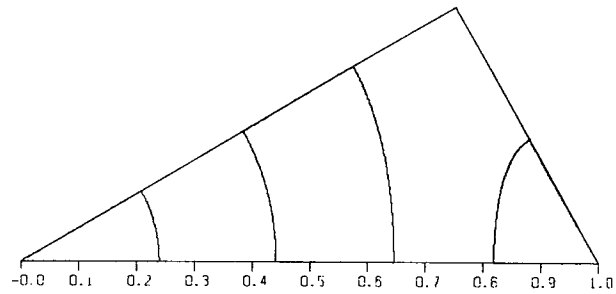

(b)

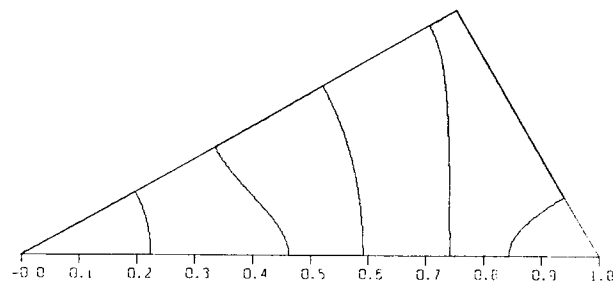

(c)

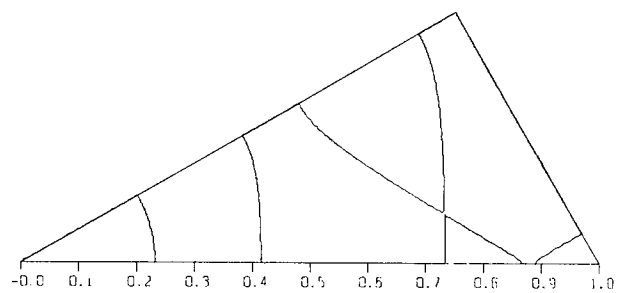

(d)

Fig. 10 — Null loci plots of H_{61} arrays: (a) uniform, (b) $(H_7*)^4$, (c) H_{19} H_7 H_7, case A and (d) $H_{19} * H_7 * H_7$, case B.

UNCLASSIFIED

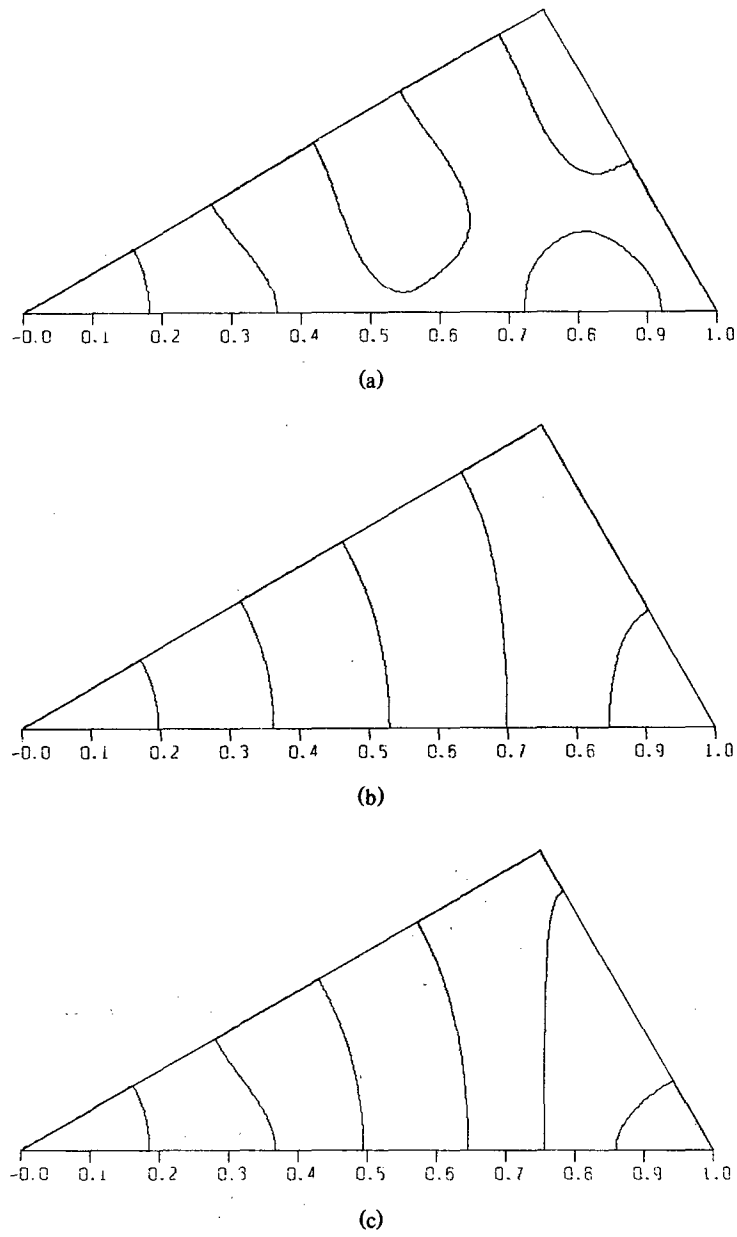

Fig. 11 — Null loci plots of H_{91} arrays: (a) uniform, (b) $(H_7{*})^5$ and (c) $H_{19} * (H_7{*})^3$

For all of the synthesized arrays, the loci of nulls away from the main beam are considerably different from those of the corresponding uniform arrays.

To understand the effect of AIE optimization on the overall array performance, it is necessary to examine the pattern topography. This is best accomplished through contour plots of power patterns in u-v space. In the following, the power contours are in 3-dB steps and are plotted in the triangular cell. Once again, the u-v space is normalized and the scale is shown along the coordinate axis only. Furthermore, contour levels are not shown for the sake of clarity; however, the levels may be readily determined from the fact that the lowest contour level shown in all plots is −39 dB.

Figures 12b and c show the patterns of a uniform H_{19} and of the H_{19} array synthesized from the convolution of two H_7 subarrays. The 3-dB beamwidth of the synthesized array is slightly larger. Notice the similarity of the pattern in Fig. 12c with the pattern in Fig. 12a which is for a uniform H_7 array. The ring-like structure of the pattern is quite apparent.

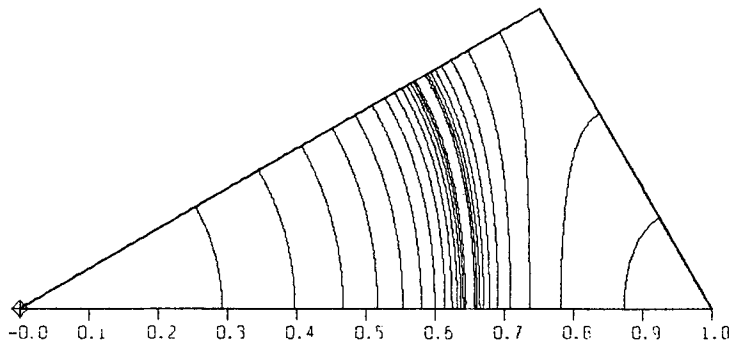

(a)

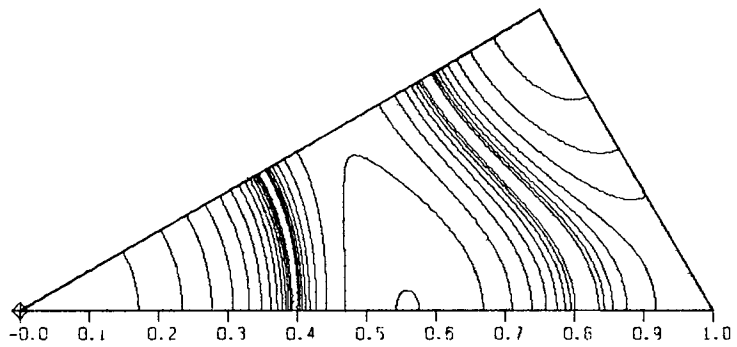

(b)

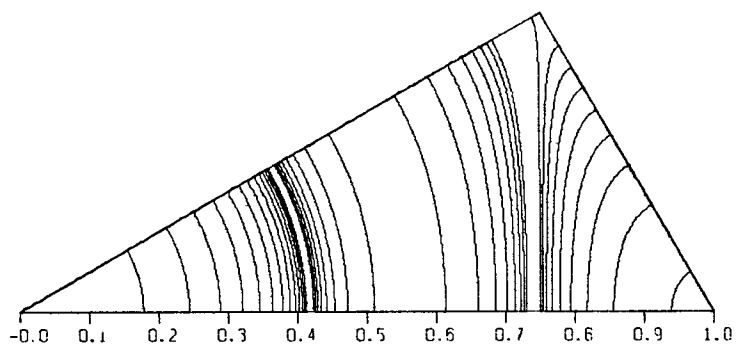

(c)

Fig. 12 — Power pattern for (a) uniform H_7, (b) uniform H_{19} and (c) $H_7 * H_7$

Patterns of H_{37} array for the cases of uniform and the two synthesized arrays are shown in Fig. 13. The near-in sidelobe level of the synthesized arrays is within 0.5 dB (greater than) of that of the uniform array. The pattern of Fig. 13b has a ring-like near-in sidelobe structure and the main beam is relatively flat. This is depicted by multiple symbols near the main beam. Also, the 3-dB beamwidth is larger. However, the pattern of Fig. 13c has 3-dB beamwidth nearly identical to that of the uniform array.

UNCLASSIFIED

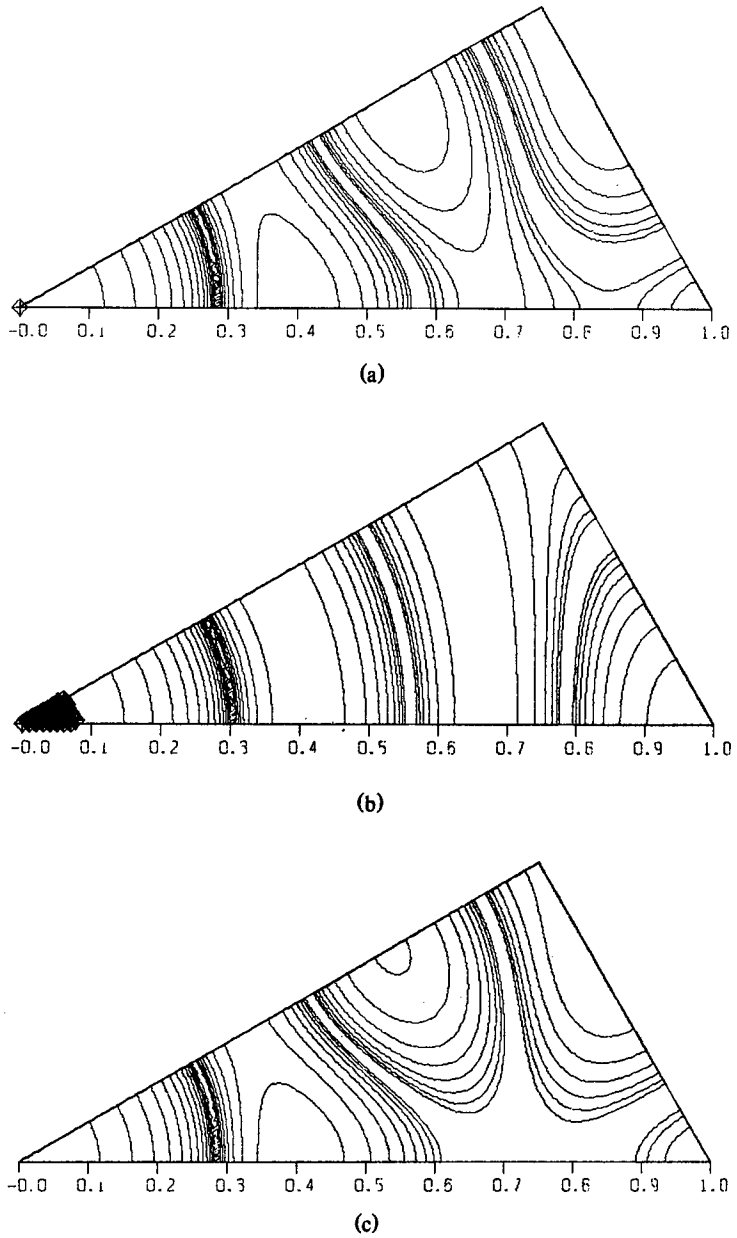

Fig. 13 — Power patterns for 37-element arrays: (a) uniform, (b) $H_7 * H_7 * H_7$, and (c) $H_{19} * H_7$

Patterns for the three designed H_{61} arrays and a uniform H_{61} array are shown in Fig. 14. The pattern in Fig. 14b is for the array synthesized with four H_7 subarrays and has a strong ring-like structure. The near-in sidelobe level is slightly below that of the uniform array shown in Fig. 14a; however, the 3-dB beamwidths are identical for the two arrays. The pattern topography of Fig. 14c near the main beam and the first sidelobe peak is nearly identical to that of the uniform array. Recall that this array is synthesized using a H_{19} array with all its zeros near the main beam. Although the first and second nulls are identical (as pointed out previously), the 3-dB beamwidth is marginally larger. The H_{61} array for which the pattern is shown in Fig. 14d is synthesized using an H_7 array with its zero near the main beam. This results in a ring-like pattern around the near-in sidelobe peak; however, the widening of the ring array from the coordinate axis may, in fact, result in a sidelobe peak near the edge of the cell and it may show up if the pattern plot was generated in smaller dB steps.

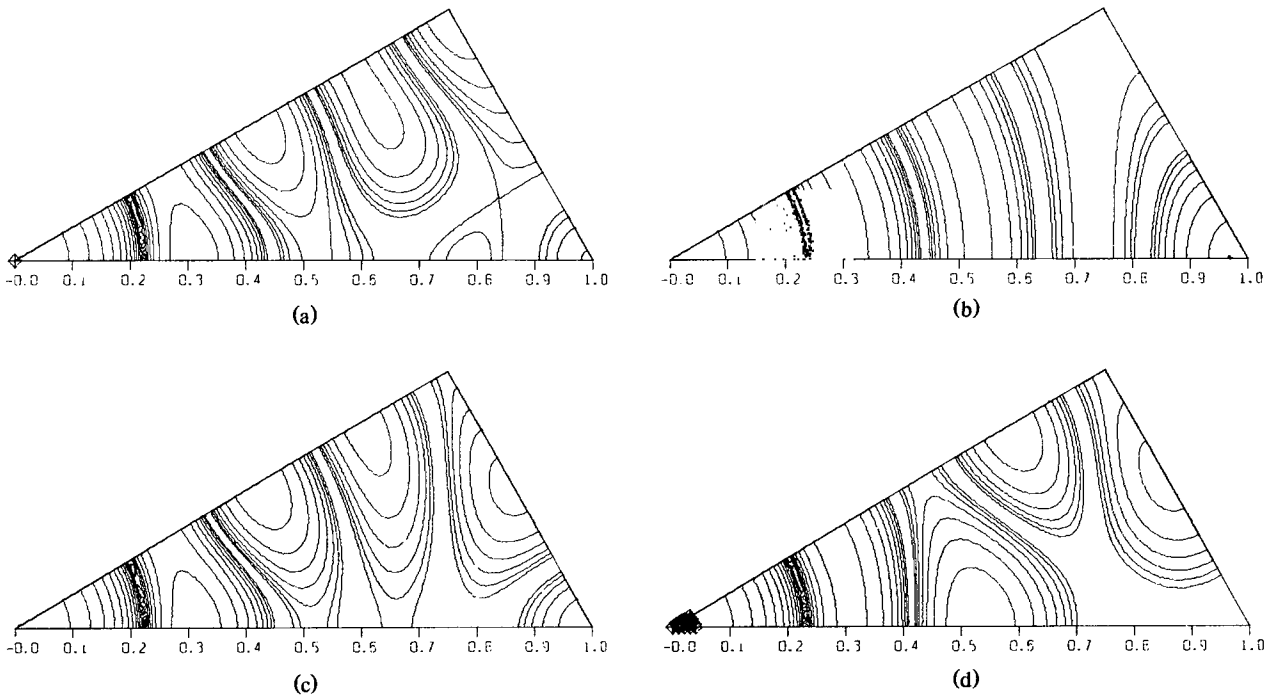

Fig. 14 — Power patterns for 61-element arrays: (a) uniform, (b) $(H_7*)^4$, (c) $H_{19} * H_7 * H_7$, case A and (d) $H_{19} * H_7 * H_7$, case B.

Shown in Fig. 15 are the patterns for H_{91} arrays: uniform, and the two arrays synthesized with H_7 and H_{19} arrays. Figure 15b shows patterns of the array generated from five H_7 subarrays which exhibit ring-like structure of an H_7 array. The 3-dB beamwidth is greater than that of the uniform array. The pattern in Fig. 15c has a sidelobe level nearly identical to that of the uniform array; and the 3-dB beamwidth is slightly larger.

Some of the important features of the pattern structure for the synthesized arrays discussed above are summarized in Table 4.

From the patterns presented in this section, the following general characteristics of the synthesized arrays may be readily identified. In all of the syntheses, the ring-like sidelobe structure near the main beam is generated in optimized arrays provided the zeros of the H_7 subarrays are near the main beam; however, this generally leads to lower AIE. Another interesting feature is that the number of sidelobe peaks in the triangular cell are less than or equal to those of corresponding uniform arrays.

CONCLUSIONS

An analysis of 7- and 19-element symmetric hexagonal arrays which form canonical arrays in the synthesis of larger arrays is carried out. Also shown are the null loci and pattern plots of uniformly excited 7-, 19-, 37-, 61- and 91- element hexagonal arrays.

The null loci of larger uniform arrays are utilized as initial data in the convolution synthesis of array of the same size with high aperture illumination efficiency. The synthesis is carried out by convolving one or more of either 7- and/or 19- element canonical arrays. The AIE of the convolved array is optimized by a hill climbing process. The aperture illumination AIE, null loci and patterns are presented for several different arrays of as large as 91 elements. The null loci and the pattern topography of each of these arrays are compared with those of the corresponding uniform arrays. Two useful features are identified. If the synthesis procedure utilizes only H_7 canonical arrays, then the main beam

UNCLASSIFIED

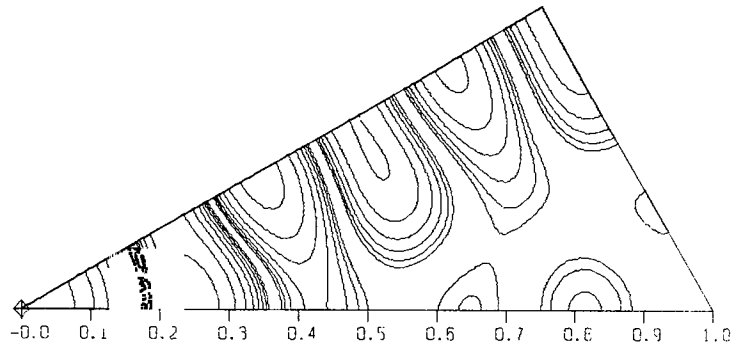

(a)

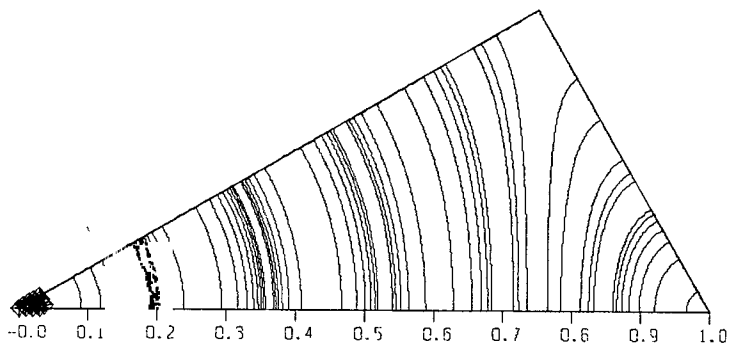

(b)

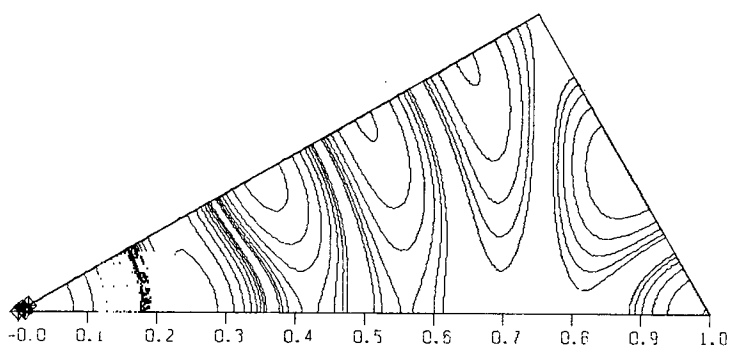

(c)

Fig. 15 — Power pattern for H_{91} arrays: (a) uniform, (b) $(H_7{*})^5$ and (c) $H_{19} * (H_7{*})^3$

Table 4—Characteristics of Pattern Structure of Various Hexagonal Arrays

		No. of sidelobe peaks in the triangular cell	Near-in sidelobe level in dB and characteristic	No. of Near-in Ring sidelobe peaks	Remarks
H_{19}	Uniform	2	$\simeq -14.5$ along u-axis		All sidelobes along the cell edge
	$H_7 * H_7$	2	$\simeq -16.5$ ring sidelobe	1	
H_{37}	Uniform	4	$\simeq -16.0$ along u-axis		All sidelobes along the cell edge
	$H_7 * H_7 * H_7$	3	$\simeq -16.5$ ring sidelobe	2	Flat main beam
	$H19 * H_7$	4	$\simeq -16.0$ along u-axis	0	All sidelobes along the cell edge
H_{61}	Uniform	6	$\simeq -16.5$ along u-axis		All sidelobes along the cell edge
	$H_7 * H_7 * H_7 * H_7$	4	$\simeq -17.0$ ring sidelobe	3	
	$H_{19} * H_7 * H_7$ Case A	5	$\simeq -16.5$ along u-axis	0	All sidelobes along the cell edge
	$H_{19} * H_7 * H_7$ Case B	4	$\simeq -17.0$ ring sidelobe	1	Flat main beam
H_{91}	Uniform	8	$\simeq -17.0$ along u-axis		All sidelobes along the cell edge
	$H_7 * H_7 * H_7 * H_7 * H_7$	5	$\simeq -17.0$ ring sidelobe	4	Flat main beam
	$H_{19} * H_7 * H_7 * H_7$	6	$\simeq -17.0$ along u-axis	0	Flat main beam All sidelobes along the cell edge

and usually the first sidelobe exhibit nearly circular locus. Synthesis of larger arrays with the H_{19} canonical array leads to patterns that have main beam null locus identical to that of the corresponding uniform array.

Aperture illumination efficiencies for syntheses involving only H_7 subarrays appear to have an asymptotic value in the range of 0.8 to 0.85. Synthesis of still larger arrays must be carried out to establish this bound conclusively. However, as it should be expected, the syntheses utilizing the H_{19} array exhibit higher AIE than the synthesis utilizing only H_7 arrays.

These convolution synthesis results, in addition to determining the maximum AIE of the convolved arrays, may provide the basis for a low-sidelobe synthesis technique. If a procedure analogous to the Taylor synthesis is used, in which the zeros of the maximum-gain configuration are pushed outward from the main beam, the starting maximum-gain configuration for the hexagonal array case may be the maximum-AIE convolved arrays.

UNCLASSIFIED

ACKNOWLEDGEMENT

The authors thank Dr. Henry J. Bilow of NRL for the use of his graphics programs.

REFERENCES

1. Ye.V. Baklanov, "Chebyshev Distribution of Currents for a Plane Array of Radiators," Radio Engrg. and Electronic Phys. 11:640-642, (1966).

2. F-I. Tseng and D.K. Cheng, "Optimum Scannable Planar Arrays with an Invariant Sidelobe Level," *Proc. IEEE* **56**, 11:1771-1778, 1968.

3. N. Goto, "Pattern Synthesis of Planar Arrays," *Electronics and Commun. in Japan* **55**, 1:68-73, 1972.

4. N. Goto, "Nonseparable Pattern of Planar Arrays," *IEEE Trans. Antennas and Propagat.* **AP-20**, 1:104-106, 1972.

5. R.S. Elliott, "Synthesis of Rectangular Planar Arrays for Sum Patterns with Ring Sidelobes of Arbitrary Topography," *Radio Science* **12**, 5:653-657, 1977.

6. N. Goto, "Pattern Synthesis of Hexagonal Planar Arrays, *IEEE Trans. Antennas and Propagat.* **AP-20**, 4:479-482, 1972.

7. N. Goto, "A synthesis of Array Antennas for High Directivity and Low Sidelobes," *IEEE Trans. Antennas and Propagat.* **AP-20**, 4:427-431, 1972.

8. D.K. Cheng and Y.K. Chen, "Optimum Planar Hexagonal Arrays," Digest of the International Symposium on Antennas and Propagation, Quebec, Canada, 335-337, 1980.

9. O. Einarsson, "Optimization of Planar Arrays," *IEEE Trans. Antennas and Propagat.* **AP-27**, 1:86-92, 1979.

10. J.P. Shelton, "Pattern-Synthesis Procedure for Regular Planar Arrays," NRL Report 8368, Feb. 1980.

11. S.R. Laxpati, "A Null Synthesis Technique for Planar Arrays," NRL Report 8478, June 1981.

12. S.R. Laxpati, "Synthesis of Planar Arrays Based on Convolution Technique," *Electronics Letters* **16**, 24:918, 1980.

13. S.R. Laxpati and J.P. Shelton, "Theory of Null Synthesis of Planar Arrays," Digest of the International Symposium on Antennas and Propagation, Los Angeles, 40-43, 1981.

14. J.P. Shelton and S.R. Laxpati, "Applications of Null Synthesis to Hexagonal Arrays," Digest of the International Symposium on Antennas and Propagation, Los Angeles, 44-47, 1981.

Appendix

RELATIONSHIP BETWEEN AIE AND THE MEAN LEVEL OF THE RANDOM SIDELOBES

An expression for the mean level of the random sidelobes of a nonuniformly excited array in terms of its aperture illumination efficiency (AIE) is derived in this appendix.

Consider an N-element array with element excitation voltages E_n, $n = 1, 2, \ldots, N$. This nonuniform illumination can be expressed as fluctuation from its mean value E_a.

$$E_n = E_a + \Delta E_n, n = 1, 2, , \ldots, N. \tag{A1}$$

The AIE of the array can be readily obtained from the directivity expression in the section on maximum AIE for convolved arrays; i.e.,

$$\text{AIE} = \eta = \frac{(\Sigma E_n)^2}{N\Sigma(E_n)^2}. \tag{A2}$$

Substitute the above expression for E_n and assume that ΔE_n are random and have zero mean. Then

$$\eta = \frac{(NE_a)^2}{N(NE_a^2 + \Sigma\Delta E_n^2)} \tag{A3}$$

Let ΔE_a^2 be the mean square value of ΔE_n. Then,

$$\eta = \frac{1}{1 + \dfrac{\Delta E_a^2}{E_a^2}} \simeq 1 - \frac{\Delta E_a^2}{E_a^2}, \tag{A4}$$

provided $\Delta E_a^2 << E_a^2$.

Note that $\Delta E_a^2/E_a^2$ is the ratio of the power in the fluctuations of the illumination to the power in the average illumination. However, if it is assumed that all the power in the fluctuations is radiated as sidelobes, the mean sidelobe level for the array with a directivity of N will be given by

$$\text{Sidelobe Ratio} = \frac{N}{\Delta E_a 2/E_a^2} = \frac{N}{1 - \eta}. \tag{A5}$$

Thus, the mean sidelobe level in dB is

$$SL = 10 \log_{10} \left(\frac{N}{1 - \eta}\right). \tag{A6}$$

By use of this expression, the mean sidelobe level for various arrays studied in this work is calculated and plotted in Fig. 6.

It should be noted that this result can also be derived using the expressions for the normalized pattern and directivity (Eq. 6.41 and 6.46 of [A1]) derived for the case of random errors in amplitude.

UNCLASSIFIED

REFERENCES

A1. R.E. Collin and F.J. Zucker, Ed., *Antenna Theory Part 1*, McGraw-Hill, Inc., New York, 227-233, 1969.